Abasic Analogues of TSAO-T as the First Sugar Derivatives That Specifically Inhibit HIV-1 Reverse Transcriptase

Sonsoles Velázquez,[§] Cristina Chamorro,[§] María-Jesús Pérez-Pérez,[§] Rosa Alvarez,[§] María-Luisa Jimeno,[§] Angel Martín-Domenech,[§] Carlos Pérez,[†] Federico Gago,[†] Erik De Clercq,[‡] Jan Balzarini,[‡] Ana San-Félix,[§] and María-José Camarasa*,[§]

Instituto de Química Médica, C.S.I.C., Juan de la Cierva 3, 28006 Madrid, Spain, Departamento de Farmacología, Universidad de Alcalá, 28871 Alcalá de Henares, Madrid, Spain, and Rega Institute for Medical Research, Katholieke Universiteit Leuven, B-3000 Leuven, Belgium

Received June 18, 1998

With the aim of assessing the role that the thymine base of TSAO-T may play in the interaction of TSAO compounds with HIV-1 reverse transcriptase (RT), we have designed, synthesized, and evaluated for their anti-HIV-1 activity a series of 3-spiro sugar derivatives substituted at the anomeric position with nonaromatic rings or with amine, amide, urea, or thiourea moieties that mimic parts or the whole thymine base of TSAO-T. Also, a dihydrouracil TSAO analogue and *O*-glycosyl 3-spiro sugar derivatives substituted at the anomeric position with methyloxy or benzyloxy groups have been prepared. Compounds substituted at the anomeric position with an azido, amino, or methoxy group, respectively, were devoid of marked antiviral activity (EC$_{50}$: 10−200 μM). However, the substituted urea sugar derivatives led to an increase in antiviral potency (EC$_{50}$: 0.35−4 μM), among them those urea derivatives that mimic most closely the intact TSAO-T molecule retained the highest antiviral activity. Also, the dihydrouracil TSAO derivative retained pronounced anti-HIV-1 activity. None of the compounds showed any anti-HIV-2 activity. The results described herein represent the first examples of sugar derivatives that interact in a specific manner with HIV-1 RT. Molecular modeling studies carried out with a prototype urea derivative indicate that a heteroaromatic ring is not an absolute requirement for a favorable interaction between TSAO-T and HIV-1 RT. Urea derivatives, which can mimic to a large extent both the shape and the electrostatic potential of a thymine ring, can effectively replace this nucleic acid base when incorporated into a TSAO molecular framework with only moderate loss of activity.

Introduction

Key targets in the search for effective drugs useful for AIDS therapy are the viral enzymes that have critical roles in the life cycle of the human immunodeficiency virus type 1 (HIV-1). One such essential enzyme is reverse transcriptase (RT).[1,2] A number of inhibitors of HIV RT have been developed.[3−5] Among them, the nonnucleoside RT inhibitors (NNRTI) represent a group of highly potent and specific inhibitors of HIV-1 replication[6,7] that interact noncompetitively with the enzyme at an allosteric nonsubstrate binding site that is distinct from, but functionally and also spatially associated with, the substrate binding site.[8−10] This particular site corresponds to a flexible, highly hydrophobic pocket that is exclusively found in the reverse transcriptase of HIV-1, and hence, NNRTIs are only inhibitory to HIV-1 and not HIV-2 or other retroviruses.[6,7]

Among NNRTIs, TSAO derivatives represent a particular and peculiar group of specific RT inhibitors, developed in our laboratories,[11,12] that are able to interfere at the interface between the p51 and p66 RT subunits. Well-defined amino acids at both the p51 and p66 RT subunits are needed for an optimum interaction

Chart 1. Chemical Structures of TSAO-T and TSAO-U
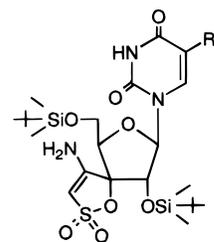
1 R = CH$_3$; TSAO-T
2 R = H ; TSAO-U

of TSAO molecules with both subunits at the same time.[12−15] Structurally TSAO are highly functionalized nucleosides. The prototype compound is [1-[2′,5′-bis-*O*-(*tert*-butyldimethylsilyl)-β-D-ribofuranosyl]thymine]-3′-spiro-5″-(4″-amino-1″,2″-oxathiole 2″,2″-dioxide) designated as TSAO-T (**1**) (Chart 1).[11b] These compounds exert their unique selectivity for HIV-1 through a specific interaction with the HIV-1 RT that, unlike the interaction of the nucleoside type of RT inhibitors, is noncompetitive with regard to the normal substrates.[16] Our experimental data strongly suggest a specific interaction of the 3′-spiro moiety of TSAO molecules with a glutamic acid residue at position 138 (Glu-138) of the p51 subunit of HIV-1 RT.[13,14,17]

Structure−activity relationship (SAR) studies within

§ C.S.I.C.
† Universidad de Alcalá.
‡ Katholieke Universiteit Leuven.

this class of compounds have revealed that stringent requirements exist with regard to the structural determinants for optimum anti-HIV activity in cell culture. The sugar part of the TSAO molecules plays a decisive and crucial role in the interaction of TSAO compounds with the target HIV-1 RT enzyme. However, the role of the base part in this interaction is yet unclear.[12] Thus, the presence of *tert*-butyldimethylsilyl (TBDMS) groups at both the C-2′ and C-5′ positions and of the unique 3′-spiro-5″-(4″-amino-1″,2″-oxathiole 2″,2″-dioxide) in nucleosides with a D-ribo configuration is a prerequisite for antiviral activity.[11b,18−20] In contrast, the nature of the heterocyclic base is less critical for anti-HIV-1 activity. The thymine moiety of TSAO-T can be replaced by a number of other pyrimidines, purines, and 1,2,3-triazoles without a marked decrease in antiviral efficacy.[11b,19−21]

As part of our ongoing program to further explore the effects of different substituents on the anti-HIV-1 activity of TSAO derivatives and, in particular, to determine the role that the nucleobase may play in this interaction, novel compounds were designed in which the sugar part of the prototype compound TSAO-T was maintained but the base part (thymine) was modified. A series of 3-spiro sugar derivatives substituted at the anomeric position with nonaromatic rings or with amine, amide, urea, or thiourea moieties derived from a systematic disassemblage of the molecular architecture of the thymine ring were prepared. The new compounds were aimed at assessing (i) the role that aromaticity and (ii) the role that different fragments mimicking parts or the thymine base of TSAO-T may play in the interaction of the TSAO functionality with the RT enzyme. Finally, for comparative purposes we also prepared *O*-glycosyl 3-spiro sugar derivatives substituted at the anomeric position with aromatic and nonaromatic lipophilic moieties such as benzyl ether or methyl ether groups, respectively.

In this paper we report the synthesis and anti-HIV-1 activity of these novel compounds.[22] The compounds described herein represent the first examples of sugar derivatives that interact in a specific manner with HIV-1 RT. To rationalize the results obtained, a theoretical investigation was undertaken to gain insight into the conformational preferences of a protoype urea derivative and its possible mode of binding to the nonnucleoside binding pocket.

Results and Discussion

Chemistry. To determine the importance of aromaticity of the base for the interaction of TSAO derivatives with HIV-1 RT, we prepared the dihydrouracil TSAO analogue **3**. Thus, treatment of TSAO uracil **2**[11b] (Scheme 1) with hydrogen in the presence of 10% Pd/C gave the dihydrouracil derivative **3** in 52% yield.

On the other hand, to assess which is the minimum fragment of the thymine moiety of the prototype compound (TSAO-T, **1**) necessary for the interaction with HIV-1 RT, we designed 3-spiro sugar derivatives bearing at the anomeric position different fragments that mimic (parts of) or the whole thymine base of TSAO-T. The 1-urea- or thiourea-substituted 3-spiro sugar derivatives were prepared by reaction of the corresponding isocyanates or isothiocyanates with the appropriate

Scheme 1
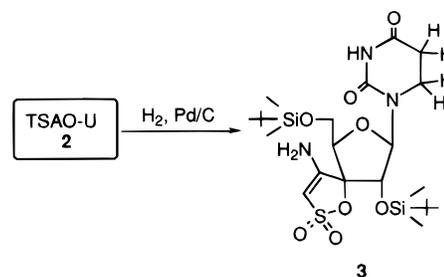
1-amino sugar intermediate **5** (Scheme 2). This intermediate was prepared by reduction of the ribosyl azide derivative **4**.[21] Initial attempts to reduce **4** by catalytic hydrogenation failed because reduction of **4** was sluggish and after 3 days only traces of the reduced product **5** were detected. However, compound **5** was obtained in almost quantitative yield when **4** was reduced using the method of Staudinger[23] for the reduction of azides. Thus, reaction of **4** with trimethylphosphine followed by treatment with saturated methanolic ammonia (to hydrolyze the phosphinimine intermediate formed) gave the ribosylamine **5** as an anomeric mixture in which the very major compound was the β anomer, as deduced from its ^{1}H NMR spectrum. Compound **5** was unstable in solution and therefore was used immediately in the next step without further purification. The instability of anomeric glycosylamines is well-documented in the literature.[24] Acetylation of **5** with Ac_2O/pyridine afforded a mixture of the two *N*-acetyl derivatives **6a** and **6b** in 20% and 23% yield, respectively. The yield obtained for the α anomer (**6a**) could be explained by mutarotation of the starting β-amine **5** to the α compound. This effect was also observed in the reaction of **5** with several isocyanates (vide infra). It should be pointed out that, as mentioned above, reduction of the β-ribofuranosylamine **4** yielded mainly the β-amine **5**, but on standing in solution, this compound mutarotates very readily to the α compound. Therefore, even when freshly prepared the anomeric amine **5** is a mixture of α and β forms. The mutarotation of other furanosyl or pyranosyl anomeric amines has been reported.[24−26]

Reaction of **5** with chlorosulfonyl isocyanate followed by treatment with aqueous $NaHCO_3$ gave the ribofuranosylurea derivatives **7a** (45% yield) and **7b** (24% yield). Acetylation of urea derivative **7b** with Ac_2O/pyridine gave the corresponding *N*-acetylurea derivative **8b** (21%). Attachment of the acetyl residue to the N′H of the urea and not to the 1-NH was established from the ^{1}H NMR spectrum by the disappearance of the broad singlet at 6.98 ppm assigned to one of the N′H$_2$ protons and the downfield shift of the broad singlet corresponding to the other N′H proton. The latter appeared at 9.55 ppm, due to the deshielding effect of the C=O of the acetyl group attached to the N′H. No modification was observed in the multiplicity of the signals corresponding to the 1-NH or to the anomeric protons, with respect to those observed for the starting **7b**.

Reaction of the amino sugar intermediate **5** with other isocyanates such as ethyl, methacryloyl, or benzoyl isocyanate in dry acetonitrile at room temperature afforded the corresponding mixtures of the α and β *N*-substituted urea derivatives **9a** and **9b** (34%), **10a** (16%) and **10b** (62%), or **11a** (10%) and **11b** (54%), respec-

Scheme 2

tively. The mixtures of anomers could be separated by chromatography except in the case of *N*-ethylurea derivatives **9a** and **9b**.

Similarly, reaction of **5** with phenyl isocyanate or phenyl isothiocyanate gave the β isomers **12b** (62.5%) or **13** (50%). In the latter reaction the corresponding α anomer was not detected, whereas only traces of **12a** were detected by ¹H NMR. Finally, reaction of **5** with 2-(methoxycarbonyl)phenyl isocyanate or 4-(methylthio)phenyl isocyanate gave the corresponding *N*-substituted urea derivatives **14a** (31%) and **14b** (33%) or **15a** (4%) and **15b** (31%).

The structures of new compounds were assigned on the basis of the corresponding analytical and spectroscopic data. Assignment of the anomeric configuration in this series was not trivial. Chemical shifts of the nuclei at the anomeric site, Δ(H-1) and Δ(C-1), will be sensitive to the configuration, but variation in the nature of the substituent at C-1 can produce overlapping ranges for both these parameters. It has been reported in the literature that for *N*-acyl-D-ribosylamines, the α anomeric proton appears at a downfield chemical shift with respect to that of the one corresponding to the β anomer.[27] In general, our compounds fulfilled this criterion, and we observed a generally larger downfield shift of the anomeric proton corresponding to the α isomer ($\delta_{H-1\alpha} > \delta_{H-1\beta}$) except in the case of compounds **11a**, **11b**, **12a**, and **12b** (see Table 1). However, this criterion must be used with caution especially when only one anomer is available as in the case of **13**.

Other parameters that have been used to establish the anomeric configuration of *N*-acylribofuranosylamines are the values of coupling constants $^3J_{1,2}$ and $^3J_{1,NH}$. It has been reported that the $J_{1,2}$ and $J_{1,NH}$ values for the α anomers are larger than the corresponding coupling constant values in the β anomers.[27,28] In our compounds the similar values observed between the α and β anomers (see Table 1) precluded the use of these parameters. Therefore, the anomeric configuration in this series of compounds was unequivocally determined by NOE experiments carried out on the major isomers **6b**, **7b**, **10b**, **11b**, **12b**, **14b**, and **15b**. Thus, for these putative β anomers irradiation of H-1 caused enhancement of the signals for both H-2 and H-4. The NOE observed between H-1 and H-4 indicated that for all these compounds both protons H-1 and H-4 are at the lower face (α face) of the furanose ring, and

therefore their anomeric configuration is β. A similar NOE experiment with compounds **8b** and **13** also indicated the β anomeric configuration.

Two additional points should be highlighted regarding the ¹H NMR data of these compounds. In the ¹H NMR spectra, *N*-acylureas **8b**, **10a**, **10b**, **11a**, and **11b** showed a strong downfield shift of the anomeric NH proton, which appeared at $\delta_{NH} = 9$ ppm. This suggests the existence of an intramolecular hydrogen bond between this NH proton and the carbonyl anchoring a *Z,E,Z*-conformation for the acylurea moiety (Chart 2). This strong downfield shift is in agreement with the values reported in the literature for other *N*-acyl-substituted urea derivatives.[29]

In compound **13** the presence of a C=S group instead of the C=O group as in **12b** causes a significant difference in the chemical shift of H-1 (Δδ ~ 1 ppm) and H-2 (Δδ ~ 0.4 ppm) with respect to these values in **12b**. It has been reported in the literature that, in general, the protons in the sulfur-containing compounds resonate further downfield than the corresponding protons in the oxygen-containing analogues.[30−32]

For comparative purposes we also prepared *O*-glycosyl 3-spiro sugar derivatives substituted at the anomeric position with methyloxy or benzyloxy groups. The methyl spiroribofuranoside **20** (Scheme 3) was prepared from 3-*C*-cyano-3-*O*-mesylribofuranoside **16**[19] in six steps. The 1,2-*O*-isopropylidene protecting group of **16** was cleaved by hydrolysis in (9:1) TFA−H₂O solution. Subsequent methylation (MeOH/H₂SO₄) and silylation (TBDMSCl/DMAP) converted the intermediate 1,2-diols to the methyl 2-silylated α- and β-(mesyloxy)nitriles **18** (57%). Treatment of **18** with DBU in acetonitrile followed by treatment with saturated methanolic ammonia afforded **19**.

Treatment of **19** with *tert*-butyldimethylsilyl chloride (TBDMSCl) gave a 1:14 mixture (deduced from ¹H NMR spectrum) of the two anomeric forms (α and β) of the 2,5-bis-*O*-silylated methyl ribofuranoside **20**. Only the major β isomer of **20** could be isolated in a pure form from the isomeric mixture. The β anomeric configuration of the major isomer was unequivocally determined by NOE experiments.

Finally, we prepared the *O*-benzyl spirofuranosides **27** and **28** (Scheme 4). Attempts to obtain the benzyl sugar derivatives by a reaction sequence similar to that described for **20** was unsuccessful. For this reason

Table 1. Selected ^{1}H NMR Spectral Data of Compounds **6−15**: Chemical Shifts (ppm), Multiplicity, and Coupling Constants (Hz)^a

compd	H-1 ($J_{1,2}$)	H-2	H-4 ($J_{4,5}$)	H-5	NH-1 ($J_{1,NH}$)	H-3′	NH$_2$-4′	others
6a	5.98 dd (6.9)	4.71 d	4.22 t (2.1)	3.89 m	7.25 bd (10)	5.72 s	6.33 bs	1.98 s, COCH$_3$
6b	5.11 dd (6.7)	4.60 d	4.03 m	4.00 m	7.85 bd (8.3)	5.59 s	6.45 bs	1.97 s, COCH$_3$
7a	5.85 dd (6.8)	4.72 d	4.28 m	3.90 m	6.68 bd (7.8)	5.72 s	6.40 bs	8.80 bs, 9.40 bs, CONH$_2$
7b	5.43 t (7.9)	4.33 d	4.14 t	3.93 m	6.30 bd (7.9)	5.67 s	6.37 bs	6.98 bs, 8.60 bs, CONH$_2$
8b	5.56 dd (8.0)	4.34 d	3.16 t (2.3)	3.92 m	9.02 bd (10.4)	5.70 s	6.38 bs	2.10 s, COCH$_3$; 9.55 bs, CON′HCO
9a^b	5.30 dd (5.2)	4.50 d	4.31 t (2.5)	3.85 m	6.36 bd (9.7)	5.70 s	6.28 bs	0.90 m, CH$_2$CH$_3$; 3.90 m, N′HCH$_2$
9b^b	5.21 t (5.0)	4.23 d	4.13 t (2.9)	3.85 m	6.42 bd (5.0)	5.63 s	6.36 bs	0.90 m, CH$_2$CH$_3$; 3.90 m, N′HCH$_2$
10a	5.95 dd (6.8)	4.76 d	4.26 m	3.92 m	9.54 bd (9.2)	5.74 s	6.32 bs	5.62 m, 5.99 m, =CH$_2$; 9.25 bs, CON′HCO
10b	5.61 dd (8.0)	4.40 d	4.22 t (2.3)	3.96 m	9.25 bd (10)	5.76 s	6.46 bs	5.75 m, 6.11 m, =CH$_2$; 9.46 bs, CON′HCO
11a	5.26 t (9.5)	4.08 d	4.23 dd (5.4, 3.6)	3.78 m	9.17 bd (9.5)	5.50 s	6.31 bs	7.57 m, 8.04 m, Ph; 9.82 bs, CON′HCO
11b	6.01 dd (6.8)	4.79 d	4.32 m	3.94 m	9.76 bd (9.46)	5.77 s	6.33 bs	7.55 m, 8.04 m, Ph; 9.76 bs, CON′HCO
12a	5.27 dd (7.1)	4.54 d	4.06 m	3.96 m	6.40 bd (7.4)	5.63 s	6.50 bs	7.00 m, 7.35 m, 7.50 m, Ph; 8.40 bs, CON′HPh
12b	6.01 dd (6.9)	4.70 d	4.23 dd (1.8, 2.5)	3.90 m	6.33 bd (9.9)	5.72 s	6.33 bs	7.00 m, Ph; 8.67 bs, CON′HPh
13	6.73 dd (6.8)	4.80 d	4.24 m	3.92 m	7.53 bd (9.2)	5.76 s	6.41 bs	7.4 m, Ph; 9.52 bs, CSN′HPh
14a	6.04 dd (6.8)	4.78 d	4.27 t	3.92 m	7.02 bd (9.6)	5.73 s	6.30 bs	3.88 s, CO$_2$CH$_3$; 7.75 m, Ph; 10.07 bs, CON′HPh
14b	5.29 dd (6.8)	4.63 d	4.10 m (2.8, 5.2)	3.97 m	7.42 bd (8.8)	5.62 s	6.33 bs	3.91 s, CO$_2$CH$_3$; 7.75 m, Ph; 10.27 bs, CONHPh
15a	6.00 dd (6.9)	4.75 d	4.23 t (2.1)	3.90 d	6.31 bd (9.8)	5.73 s	6.35 bs	2.42 s, SCH$_3$; 7.30 m, Ph; 8.68 bs, CON′HPh
15b	5.26 dd (7.1)	4.56 d	4.06 m (2.7, 4.6)	3.93 m	6.36 bd (8.9)	5.62 s	6.44 bs	2.43 s, SCH$_3$; 7.30 m, Ph, 8.35 bs, CON′HPh

^{a} (CD$_3$)$_2$CO at 200 MHz. ^{b} CDCl$_3$ at 200 MHz.

Chart 2

8b, R = CH$_3$

11a,11b, R = Ph

10a,10b

Scheme 3

16

17 R = H

18 R = Si

19 R = H

20 R = Si

(i) 9:1 TFA/H$_2$O; (ii) MeOH/H$_2$SO$_4$;
(iii) TBDMSCl/DMAP; (iv) DBU; (v) NH$_3$/MeOH;
(vi) TBDMSCl/DMAP

compounds **27** and **28** were prepared following our reported procedure for the synthesis of the ribo- and xylofuranosyl TSAO pyrimidine nucleosides.[11b] Treatment of the ulose **22**, prepared by oxidation of **21**[33] (pyridinium dichromate/Ac$_2$O/CH$_2$Cl$_2$),[34] with sodium cyanide in a diethyl ether/water two-phase system in the presence of NaHCO$_3$ yielded, after mesylation (mesyl chloride/pyridine) of the two epimeric cyanohydrins (**23** and **24**), a mixture of the respective *O*-benzyl ribo and xylo cyanomesylates **25** (15%) and **26** (60%). Treatment of **25** or **26** with DBU in acetonitrile gave the 3-spiro derivatives **27** (50%) and **28** (70%). Assignment of the structures of these ribo and xylo derivatives was made by comparison of their spectroscopic data with those of other ribo and xylo 3-cyanomesylates and spiro derivatives of this series

whose structures have been unequivocally determined.[11b,19−21,35,36]

Structural Features. The acyclic substituent at the anomeric position of the most active acylureas **8b** and **10b** (vide infra) could exist in different conformations (Chart 3). The spectroscopic data were only compatible with six-membered hydrogen-bonded pseudocycle conformer II but not with conformers I or III. In addition, in compound **10b** conformer II can have two orientations

Scheme 4

(i) Pyridinium dichromate /Ac₂O/CH₂Cl₂
(ii) NaCN/Et₂O/H₂O/NaHCO₃
(iii) MsCl/Py
(iv) DBU/acetonitrile
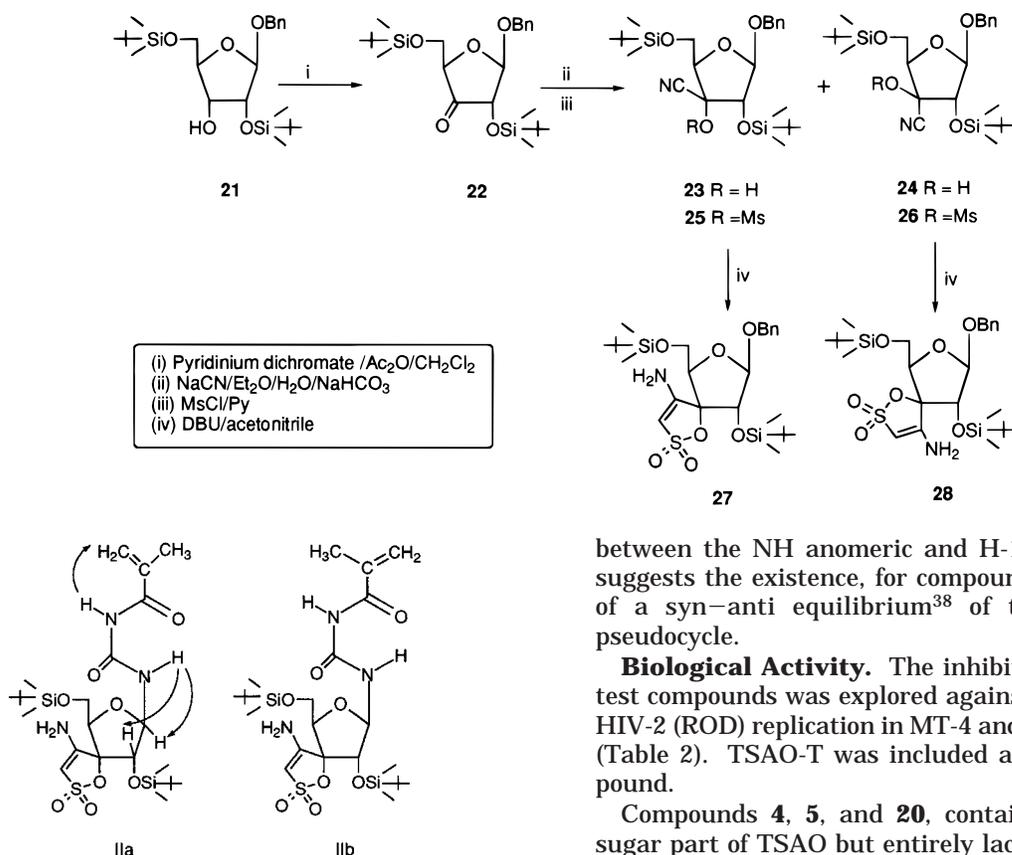
Figure 1. NOEs observed for compound **10b** upon irradiation of anomeric NH and N′H protons.

Chart 3. Conformations for acylureas **8b** and **10b**

8b, R = CH₃
10b, R = —C(=CH₂)CH₃
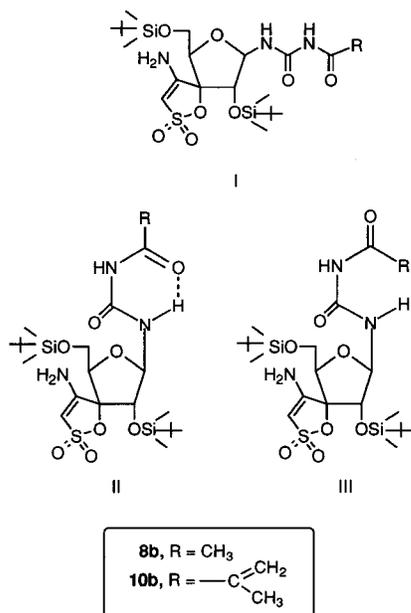
of the R substituent (Figure 1). The predominant orientation (in acetone) for this compound was unequivocally determined by a selective NOE experiment.[37] Thus, irradiation of the NH anomeric caused enhancements of the signals for H-1 and H-2 sugar protons. Likewise, irradiation of the N′H proton influenced the signals for =CH₂. These results were only compatible with conformer IIa. Moreover, the NOE observed

between the NH anomeric and H-1 and H-2 protons suggests the existence, for compound **10b**, in solution of a syn–anti equilibrium[38] of the six-membered pseudocycle.

Biological Activity. The inhibitory activity of the test compounds was explored against HIV-1 (III$_B$) and HIV-2 (ROD) replication in MT-4 and CEM cell cultures (Table 2). TSAO-T was included as a reference compound.

Compounds **4**, **5**, and **20**, containing the silylated sugar part of TSAO but entirely lacking the base part (replaced by an azido, amino, or methoxy group, respectively), were devoid of marked antiviral activity (EC$_{50}$: >200, >10, and 21 μM). However, extending the amino group in the C-1 β anomeric position of the sugar part with additional functional groups led to an increase in antiviral potency. Whereas **6b** showed an EC$_{50}$ of 2.6 and 2.8 μM against HIV-1 (CC$_{50}$: 13 μM in MT-4 cells), **8b** was active at 0.89 and 0.65 μM (CC$_{50}$: 15–26 μM). Compound **10b** had a slightly further improved antiviral activity (EC$_{50}$: 0.59 and 0.56 μM) but also increased toxicity (CC$_{50}$: 6.1–8.6 μM).

As a rule, the corresponding α anomeric derivatives were virtually devoid of significant antiviral activity among those compounds that had an aliphatic extension at the C-1 carbon of the sugar part. However, among the aromatic extensions of the sugar moiety, this property proved only to be the case when **11b** was compared with **11a**. Surprisingly, the β anomeric **12b** proved to be 10–12-fold less active than its corresponding α anomeric derivative. Also, **14a**, **14b** and **15a**, **15b** were comparably active against HIV-1 replication in both CEM and MT-4 cell lines. Their EC$_{50}$ values ranged between ≥2 and 5.3 μM, but the CC$_{50}$ ranged from 3.8 to 29 μM. Finally, both ribo and xylo derivatives of the benzyl-substituted compounds **27** and **28** were endowed with antiviral activity (EC$_{50}$: 4.6 to ≥6.4 μM) and cytotoxicity (CC$_{50}$: 11–13 μM).

As a rule, none of the compounds had any anti-HIV-2 activity, which is consistent with the complete lack of anti-HIV-2 activity of the TSAO derivatives (i.e., TSAO-T). Also, akin to TSAO-T, **8b**, **10b**, **12a**, **15a**, and **15b** were not inhibitory to Glu-B138 Lys RT mutant virus replication indicating that the interaction with Glu-138 of the enzyme is most likely preserved in the TSAO

Table 2. Antiviral Activity of TSAO Derivatives against HIV-1 and HIV-2 in CEM and MT-4 Cell Cultures

| | EC$_{50}$ (μM)[a] | | | | CC$_{50}$ (μM)[b] | |
| | MT-4 | | CEM | | | |
compd	HIV-1	HIV-2	HIV-1	HIV-2	MT-4	CEM
2[c]	0.18 ± 0.04	>20			13 ± 0.9	
3	0.92 ± 0.10	>2	0.31 ± 0.2		21 ± 0.9	19 ± 0.2
4	>200	>200	>200	>200	>200	>200
5	>10	>10	>10	>10	21 ± 0.4	16 ± 9.7
6a	>8	>8	≥8	>8	16 ± 1.4	
6b	≥8	>8	2.6 ± 0.8	>8	13 ± 1.4	
7a	>250	>250	57 ± 11	>50	>250	203 ± 66
7b	124 ± 9.2	>250	90 ± 35	>50	≥250	≥250
8b	0.89 ± 0.13	>10	0.65 ± 0.07	>10	26 ± 21	15 ± 3.7
9a + 9b	>10	>10	>10	>10	19 ± 2.7	20 ± 1.1
10a	>1.3	>1.3	>6.5	>6.5	2.7 ± 0.02	6.4 ± 2.2
10b	0.59 ± 0.02	>6.5	0.56 ± 0.34	>6.5	8.6 ± 4	6.1 ± 1.1
11a	>250	>250	>250	>250	≥250	24 ± 4.6
11b	16 ± 9.3	>50	7.0 ± 2.6	>50	90 ± 6.7	48 ± 0.8
12a	0.59 ± 0.2	>2	0.65 ± 0.02	>2	4.3 ± 0.1	4.2 ± 0.4
12b	5.1 ± 0.7	>10	≥10	>10	14 ± 1.3	10 ± 1.1
13	>2	>2	≥2	>2	3.7 ± 0.1	4.1 ± 0.4
14a	5.3 ± 2.7	>10	4.5 ± 0.7	>10	26 ± 2.5	22 ± 1.7
14b	3.1 ± 2.3	>2	≥2	>2	17 ± 1.0	3.8 ± 1.4
15a	4.2 ± 0.8	>10	>2	>2	17 ± 0.4	6.4 ± 2.5
15b	21 ± 5.4	>10	5.0 ± 0.0	>10	29 ± 3.5	22 ± 0.9
20	21 ± 8.5	>200			>200	
27	4.9 ± 2.1	>6.4	≥6.4	>6.4	12 ± 1.9	11 ± 0.64
28	4.6 ± 2.4	>6.4	≥6.4	>6.4	13 ± 1.8	11 ± 0.96
TSAO-T	0.06 ± 0.03	>20	0.06 ± 0.01	>20	14 ± 2	

[a] 50% effective concentration, or concentration required to protect 50% of the virus-infected cells against destruction by the virus. [b] 50% cytostatic concentration, or concentration required to reduce the viability of mock-infected cells by 50%. [c] Data taken from ref 12b.

derivatives modified at the base part. It may not be surprising that **8b** and **10b**, which mimic mostly the intact TSAO molecule [with base ring opening between N-1 and C-6 (for **10b**) or C-6 and C-5 (lacking the C-6 carbon atom) (for **8b**)], retained the highest antiviral activity. This may perhaps indicate that the functional groups present in the intact base and in the ring-opened forms of TSAO (**8b**, **10b**) are required for interaction with RT. Also, the comparable anti-HIV-1 activity of the dihydrouracil TSAO derivative **3** and the uracil TSAO derivative **2** suggests that an aromatic entity on C-1 of the sugar part is not an absolute requirement for the interaction with the enzyme and is in agreement with the findings for the open-ring TSAO structures.

Modeling. To rationalize the biological results obtained, a theoretical investigation was undertaken to gain insight into the conformational preferences of a prototype urea derivative (compound **10b**) and its mode of interaction with the nonnucleoside binding pocket that may reveal potential interaction points between the NNRTIs binding pocket of the enzyme and the different active molecules.

The intramolecular hydrogen bond (Chart 2) stabilizes conformer I of compound **10b** in vacuo over all the other possible conformers (Table 3). The degree of similarity with the thymine ring, however, is maximal (62%) for conformer III, in which there is no such hydrogen bond.

The AutoDock calculations consistently placed the thymine ring immediately above the plane of Tyr-A318, in a cavity delineated by the side chains of residues Leu-A100, Lys-A103, Val-A106, and Leu-A234 and the carbonyl groups of Lys-A101, His-A235, and Pro-A236. This is in agreement with the common finding of an aromatic ring filling this part of the cavity in the complexes of RT with other inhibitors.[8-10] The orientations suggested by the docking program (Figure 2a),

however, were incompatible with what is known from previous structure−activity[11,12,16,18−21] and modeling studies.[39] Most importantly, since the N-1 atom of thymine is attached to the C-1′ atom of the ribose, this ring atom must be positioned such that it allows location of the rest of the structure in the binding site so as to place the exocyclic amino group on the spiro ring in a suitable orientation for establishing an intermolecular hydrogen bond with the side chain of Glu-B138. Indirect support for this specific interaction has been recently gained from work on TSAO analogues modified on the spiro system.[17,39] Besides, the fact that the N-3 position has been linked to rather long substituents (AZT, etc.)[19,40] without a great loss of potency may indicate that this ring atom is facing the proposed entrance to the pocket, namely, the channel between Pro-A236 and the A225-A226 and A105-A106 loops.[41] Consequently, we favor the view that the thymine ring of TSAO-T is situated in this binding pocket in the orientation shown in Figure 2b. Calculation and display of the molecular electrostatic potential in this region of the enzyme binding site (data not shown) reveal a highly negative potential above the phenyl ring of Tyr-A318 as a result of electrostatic focusing.[42] On the other hand, the positive electrostatic potential of many bound inhibitors is most prominent around the edges of the heteroaromatic rings that point toward the faces of the aromatic rings of both Tyr-A318 and Trp-A229. We therefore believe that the ensuing electrostatic complementarity is important for ligand orientation and for enhanced binding affinity. In the case of TSAO-T, the carbonyl oxygen at the C-4 position of the thymine ring gives rise to a globular region of negative potential in the midst of an otherwise positive region. This may be the reason AutoDock does not select for the binding orientation that is most in consonance with our current

Table 3. Optimized Geometries of N^1-Methylthymine and Selected Conformers of the Urea Part of Compound **10b**
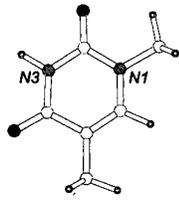
Conformer	ΔE (kcal mol^{-1})[a]	Similarity index[b]
I	-	-0.37
II	14.4	-0.18
III	11.9	0.62
IV	11.9	0.57

[a] Energy values are given with respect to conformer I. [b] Similarity with respect to N^1-methylthymine, as assessed with ASP.[48]

working model.[43] On the other hand, of all the possible conformers of **10b**, the one that AutoDock places in this binding pocket is that resembling most closely the thymine ring (conformer III, Table 3), as assessed by a similarity index of 0.62. In this conformation, the intramolecular hydrogen bond is broken, and the accompanying energy penalty ($\sim$12 kcal mol^{-1} in vacuo) may account for the loss of affinity of this compound, in comparison with TSAO-T, for the NNRTIs binding pocket. Further modifications of the thymine ring are currently in progress to test these hypotheses.

Conclusions

A close interaction with Tyr-A318 at the bottom of the hydrophobic binding site is maintained in all the X-ray complexes reported to date between RT and NNRTIs, in most cases involving an aromatic moiety. From the present results it would appear that a heteroaromatic ring is not an absolute requirement in order to get a favorable interaction in this region of the binding pocket. Urea derivatives, which can mimic to a large extent both the shape and the electrostatic potential of a thymine ring, can effectively replace this nucleic acid base when incorporated into the TSAO

molecular framework with only a moderate loss of activity. As shown in this work, the abasic TSAO analogue **10b** is just 1 order of magnitude less active than the prototype TSAO-T, and our calculations suggest that this may be due to the energy penalty involved in breaking the intramolecular hydrogen bond in order to adopt a conformation suitable for binding.

The differences in activity found among the TSAO analogues reported in this series can be explained by taking into account their distinct capability to interact with the hydrophobic pocket bounded by Tyr-A318. The most active compounds of this series (compounds **10b**, **8b**, and **12a**) are those large enough to fill this pocket and interact with hydrophobic residues Leu-A100, Val-A106, Pro-A236, and Tyr-A318. Smaller compounds (**6**, **7**) cannot give rise to all of these interactions and larger ones (**11**, **14**, and **15**) may gain limited access to the bottom of this cavity because of occupancy of part of the proposed entrance[44] between Pro-A225 and Pro-A236. In both cases the net result would be a decrease in activity.

Experimental Section

Chemical Procedures. Microanalyses were obtained with a Heraeus CHN-O-RAPID instrument. ^{1}H NMR spectra were recorded with a Varian Gemini, a Varian XL-300, and a Bruker AM-200 spectrometer operating at 300 and 200 MHz and a Varian Unity 500 spectrometer operating at 498.84 MHz with Me$_4$Si as internal standard. ^{13}C NMR spectra were recorded with a Bruker AM-200 spectrometer operating at 50 MHz, with Me$_4$Si as internal standard. IR spectra were recorded with a Shimadzu IR-435 spectrometer. Analytical TLC was performed on silica gel 60 F$_{254}$ (Merck). Separations on silica gel were performed by preparative centrifugal circular thin-layer chromatography (CCTLC) on a Chromatotron (Kiesegel 60 PF 254 gipshaltig (Merck)), layer thickness 1 mm, flow rate 5 mL/min. Flash column chromatography was performed with silica gel 60 (230–400 mesh) (Merck).

[1-[2′,5′-Bis-O-($tert$-butyldimethylsilyl)-β-D-ribofuranosyl]-5,6-dihydrouracil]-3′-spiro-5″-(4″-amino-1″,2″-oxathiole 2″,2″-Dioxide) (3). Compound **2**[11b] (0.11 g, 0.20 mmol) was dissolved in MeOH (1 mL) and hydrogenated in the presence of 10% Pd/C (0.06 g) at 30 psi at 30 °C until disappearance of the starting material. The mixture was filtered and evaporated. The residue was purified by CCTLC on the chromatotron (CH$_2$Cl$_2$–ethyl acetate, 7:1) to give **3** (0.06 g, 52%) as an amorphous solid: ^{1}H NMR (CDCl$_3$, 300 MHz) δ 2.68 (m, 2H, H-5), 3.59 (m, 1H, H-6a), 3.67 (m, 1H, H-6b), 3.91 (m, 2H, H-5′), 4.23 (pt, 1H, H-4′, $J_{4',5'}$ = 3.18 Hz), 4.53 (d, 1H, H-2′), 5.57 (s, 1H, H-3″), 5.59 (d, 1H, H-1′, $J_{1',2'}$ = 7.6 Hz), 5.59 (bs, 2H, NH$_2$-4″), 8.22 (bs, 1H, NH-3). Anal. (C$_{23}$H$_{43}$N$_3$O$_8$SSi$_2$) C, H, N, S.

[[2,5-Bis-O-($tert$-butyldimethylsilyl)-D-ribofuranosyl]-amine]-3-spiro-5′-(4′-amino-1′,2′-oxathiole 2′,2′-Dioxide) (5). To a solution of azide **4**[21] (0.2 g, 0.4 mmol) in dry THF (5 mL) was added a 1 M solution of trimethylphosphine in THF (0.6 mL, 0.6 mmol). The mixture was stirred at room temperature for 20 min and then evaporated to dryness. The residue was dissolved in methanol (6 mL) and treated with saturated methanolic ammonia (6 mL) at room temperature for 3 h. The solvent was evaporated to dryness, and the residue was coevaporated with dry acetonitrile (2 × 6 mL) to give the amino sugar **5** (quantitative yield) which was used inmediately in the next step without further purification. **5** was a mixture of α and β anomers in which the β anomer was the very major compound. ^{1}H NMR ((CD$_3$)$_2$CO, 500 MHz) β-anomer δ 3.90 (m, H-5), 4.1 (t, H-4, $J_{4,5}$ = 2.5 Hz), 4.25 (d, H-2), 5.25 (t, H-1, $J_{1,2}$ = 6.8 Hz), 5.62 (s, H-3′), 6.35 (bt, NH$_2$-1), 6.42 (bs, NH$_2$-4″); α anomer δ 2.25 (bd, NH$_2$-1, $J_{1,NH}$ = 2.2 Hz), 3.86 (m, H-5), 4.01 (d, H-2), 4.07 (t, H-4, $J_{4,5}$ = 2.8 Hz), 4.54 (m, H-1, $J_{1,2}$ = 7.2 Hz), 5.62 (s, H-3′), 6.22 (bs, NH$_2$-4″).
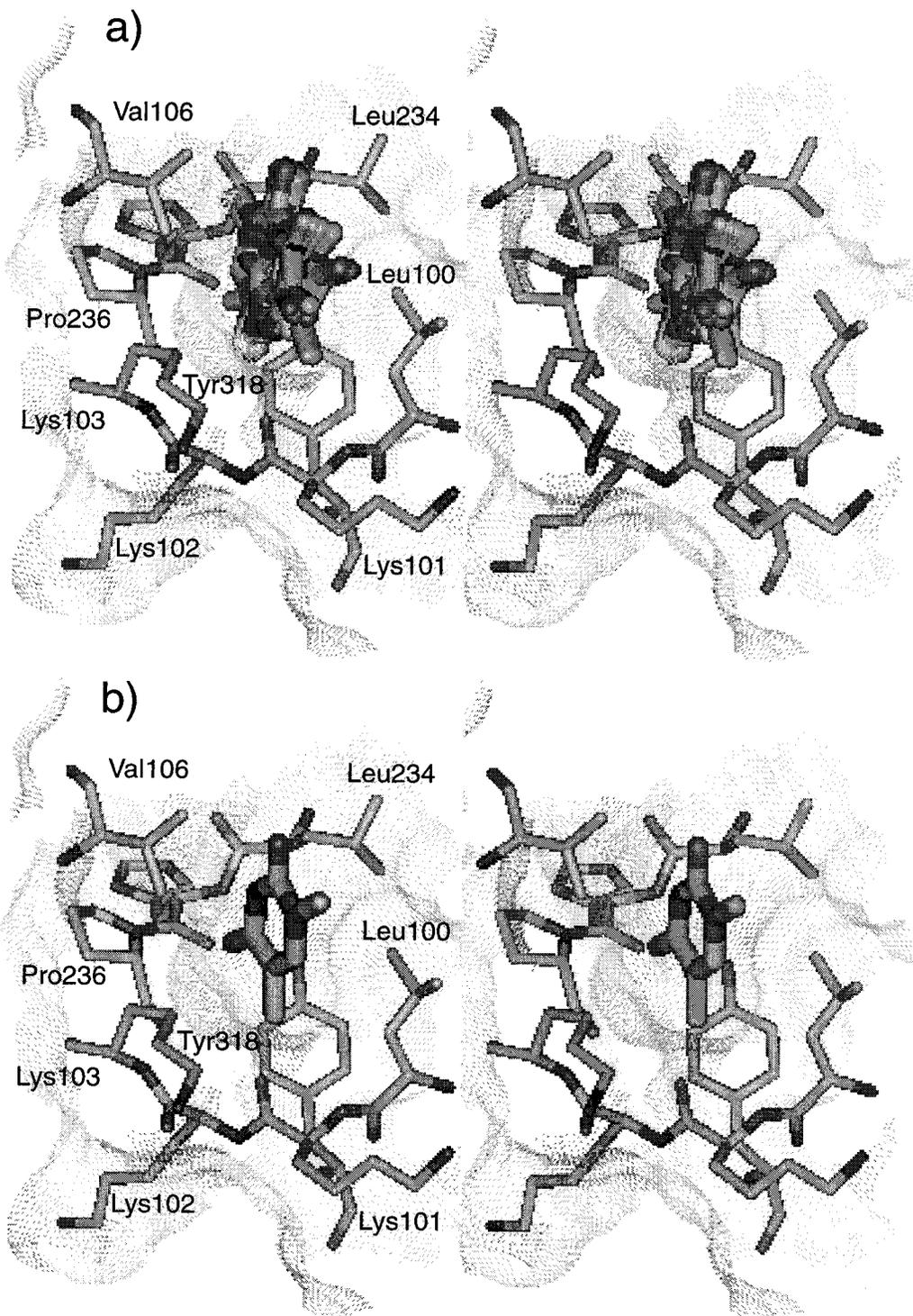
Figure 2. (a) Stereoview of the different binding orientations suggested by AutoDock for a thymine ring in part of the nonnucleoside binding pocket. Amino acid residues shown are Leu-100, Lys-101, Lys-102, Lys-103, Val-106, Leu-234, His-235, Pro-236, and Tyr-318 of the p66 palm domain of HIV-1 reverse transcriptase. Hydrogen atoms are not displayed for clarity. (b) Stereoview of the binding orientation proposed for the thymine ring of TSAO-T based on the available structure−activity relationship data.

[*N*-Acetyl-[2,5-bis-*O*-(*tert*-butyldimethylsilyl)-α- and -β-D-ribofuranosyl]amine]-3-spiro-5′-(4′-amino-1′,2′-oxathiole 2′,2′-Dioxide) (6a and 6b). To a solution of **5** (0.2 g, 0.4 mmol) in pyridine (3 mL) was added acetic anhydride (0.26 mL). The reaction mixture was kept for 17 h at room temperature and then evaporated to dryness. The residue was dissolved in dichloromethane (50 mL) and washed successively with 0.1 N HCl (10 mL) and water (2 × 10 mL). The organic layer was dried (Na₂SO₄), filtered, and evaporated to dryness. The residue was purified twice by CCTLC on the chromatotron (hexane−ethyl acetate, 3:1; then CH₂Cl₂−ethyl acetate, 4:1).

The fastest moving band gave **6a** as a white foam (0.04 g, 20%): [α]$_D$ +44.60 (*c* 1, chloroform). Anal. (C$_{21}$H$_{42}$N$_2$O$_7$SSi$_2$) C, H, N, S.

The slowest moving band gave **6b** (0.05 g, 23%) as a white foam: [α]$_D$ +8.80 (*c* 0.2, chloroform); ^{13}C NMR ((CD$_3$)$_2$CO, 50 MHz) δ 25.93, 26.17 (tBu), 63.57 (C-5), 73.77 (C-2), 79.51 (C-3′), 84.3 (C-4), 92.37 (C-1), 95.13 (C-3), 152.36 (C-4′), 170.35 (C=O). Anal. (C$_{21}$H$_{42}$N$_2$O$_7$SSi$_2$) C, H, N, S.

[*N*-[2,5-Bis-*O*-(*tert*-butyldimethylsilyl)-α- and -β-D-ribofuranosyl]urea]-3-spiro-5′-(4′-amino-1′,2′-oxathiole 2′,2′-Dioxide) (7a and 7b). To a cooled (−15 to −20 °C) solution

of ribofuranosylamine **5** (0.2 g, 0.4 mmol) in dry acetonitrile (12 mL) was added chlorosulfonyl isocyanate (0.035 mL, 0.4 mmol) in the absence of humidity. The resulting mixture was stirred at −20 °C until **5** disappeared, then neutralized (NaHCO₃), and evaporated to dryness. The residue was dissolved in isobutyl alcohol (20 mL) and washed with water (2 × 10 mL). The organic layer was dried (Na₂SO₄), filtered, and evaporated to dryness. The residue was purified by CCTLC on the chromatotron (CH₂Cl₂−acetone, 60:2) to give 0.15 g (71.5%) of the ribofuranosylureas **7a** and **7b**. This isomeric mixture was purified by CCTLC on the chromatotron (CH₂Cl₂−MeOH, 5:1). The fastest moving band gave **7a** (0.095 g, 45%) as a white foam: [α]$_D$ +24 (*c* 0.2, methanol). Anal. (C₂₀H₄₁N₃O₇SSi₂) C, H, N, S.

The slowest moving band gave **7b** (0.051 g, 24%) as an amorphous solid: [α]$_D$ +7.33 (*c* 0.7, methanol); ¹³C NMR [(CD₃)₂CO, 50 MHz] δ 26.09, 26.45 (tBu), 65.14 (C-5), 76.86 (C-2), 84.17, 84.34 (C-3′, C-4), 92.21 (C-1), 93.81 (C-3), 152.85, 156.97 (CONH₂, C-4′). Anal. (C₂₀H₄₁N₃O₇SSi₂) C, H, N, S.

[*N*-Acetyl-*N*-[2,5-bis-*O*-(*tert*-butyldimethylsilyl)-β-D-ribofuranosyl]urea]-3-spiro-5′-(4′-amino-1′,2′-oxathiole 2′,2′-Dioxide) (8b). Compound **7b** (0.1 g, 0.19 mmol) was acetylated as described for **6a** and **6b**. Purification of the residue by CCTLC on the chromatotron (hexane−ethyl acetate, 1:1) gave **8b** (0.023 g, 21%) as a white foam. Anal. (C₂₂H₄₃N₃O₈SSi₂) C, H, N, S.

Reaction of Ribofuranosylamine 5 with Isocyanates and Isothiocyanates. General Procedure for the Synthesis of *N*-Substituted Ureas and Thioureas 9−15. A mixture of ribofuranosylamine **5** (0.2 g, 0.4 mmol), dry acetonitrile (5 mL), and the appropiate isocyanate or isothiocyanate (0.06 mmol) was stirred at room temperature overnight. After evaporation of the solvent, the residue was purified by CCTLC on the chromatotron. The chromatography eluent, yield, and [α]$_D$ values of the isolated products (**9−15**) are indicated below for each reaction.

[*N*-[2,5-Bis-*O*-(*tert*-butyldimethylsilyl)-α- and -β-D-ribofuranosyl]-*N*-ethylurea]-3-spiro-5′-(4′-amino-1′,2′-oxathiole 2′,2′-Dioxide) (9a and 9b). The general procedure was followed with ethyl isocyanate. Chromatography with hexane−ethyl acetate (4:1) afforded 0.076 g (34%) of a 1:1 mixture of **9a** and **9b**. Anal. (C₂₂H₄₅N₃O₇SSi₂) C, H, N, S.

[*N*-[2,5-Bis-*O*-(*tert*-butyldimethylsilyl)-α- and -β-D-ribofuranosyl]-*N*-methacryloylurea]-3-spiro-5′-(4′-amino-1′,2′-oxathiole 2′,2′-Dioxide) (10a and 10b). The general procedure was followed with methacryloyl isocyanate. Chromatography first with CH₂Cl₂−MeOH (100:1) and then with hexane−ethyl acetate (2:1) afforded from the fastest moving band 0.15 g (62%) of **10b** as a foam: [α]$_D$ −17.8 (*c* 0.4, chloroform). Anal. (C₂₄H₄₅N₃O₈SSi₂) C, H, N, S.

The slowest moving band gave **10a** (0.039 g, 16%) as a foam: [α]$_D$ +57.8 (*c* 0.6, chloroform). Anal. (C₂₄H₄₅N₃O₈SSi₂) C, H, N, S.

[*N*-Benzoyl-*N*-[2,5-bis-*O*-(*tert*-butyldimethylsilyl)-α- and -β-D-ribofuranosyl]urea]-3-spiro-5′-(4′-amino-1′,2′-oxathiole 2′,2′-Dioxide) (11a and 11b). Isocyanate: benzoyl isocyanate. Chromatography first with hexane−ethyl acetate (1:1) and then with CH₂Cl₂−MeOH (20:1) gave from the fastest moving band 0.14 g (54%) of **11b** as an amorphous solid: [α]$_D$ +62.3 (*c* 0.1, chloroform). Anal. (C₂₇H₄₅N₃O₈SSi₂) C, H, N, S.

The slowest moving band gave **11a** (0.025 g, 10%) as an amorphous solid: [α]$_D$ −40.1 (*c* 0.1, chloroform). Anal. (C₂₇H₄₅N₃O₈SSi₂) C, H, N, S.

[*N*-[2,5-Bis-*O*-(*tert*-butyldimethylsilyl)-α- and -β-D-ribofuranosyl]-*N*-phenylurea]-3-spiro-5′-(4′-amino-1′,2′-oxathiole 2′,2′-Dioxide) (12a and 12b). Isocyanate: phenyl isocyanate. Chromatography with CH₂Cl₂−acetone (60:1) afforded from the fastest moving band 0.15 g (62.5%) of **12b** as a foam: [α]$_D$ +0.5 (*c* 0.5, chloroform). Anal. (C₂₆H₄₅N₃O₇SSi₂) C, H, N, S.

The slowest moving band gave **12a** (0.015 g, 6.2%) as a foam: [α]$_D$ −0.06 (*c* 0.45, chloroform). Anal. (C₂₆H₄₅N₃O₇SSi₂) C, H, N, S.

[*N*-[2,5-Bis-*O*-(*tert*-butyldimethylsilyl)-β-D-ribofuranosyl]-*N*-phenylthiourea]-3-spiro-5′-(4′-amino-1′,2′-oxathiole 2′,2′-Dioxide) (13). The general procedure was followed with phenyl isothiocyanate. Chromatography with CH₂Cl₂−acetone (200:1) gave **13** (0.13 g, 50%) as an amorphous solid: [α]$_D$ +0.5 (*c* 0.5, chloroform). Anal. (C₂₆H₄₅N₃O₆S₂Si₂) C, H, N, S.

[*N*-[2,5-Bis-*O*-(*tert*-butyldimethylsilyl)-α- and -β-D-ribofuranosyl]-*N*-(2-(methoxycarbonyl)phenyl)urea]-3-spiro-5′-(4′-amino-1′,2′-oxathiole 2′,2′-Dioxide) (14a and 14b). Isocyanate: 2-(methoxycarbonyl)phenyl isocyanate. Chromatography twice with hexane−ethyl acetate (2:1) gave from the fastest moving band 0.09 g (33%) of **14b** as a foam: [α]$_D$ −9.53 (*c* 0.8, chloroform). Anal. (C₂₈H₄₇N₃O₉SSi₂) C, H, N, S.

The slowest moving band gave **14a** (0.085 g, 31.5%) as a foam: [α]$_D$ +53.22 (*c* 0.4, chloroform). Anal. (C₂₈H₄₇N₃O₉SSi₂) C, H, N, S.

[*N*-[2,5-Bis-*O*-(*tert*-butyldimethylsilyl)-α- and -β-D-ribofuranosyl]-*N*-(4-(methylthio)phenyl)urea]-3-spiro-5′-(4′-amino-1′,2′-oxathiole 2′,2′-Dioxide) (15a and 15b). Isocyanate: 4-(methylthio)phenyl isocyanate. Chromatography with CH₂Cl₂−MeOH (20:1) gave from the fastest moving band **15a** (0.01 g, 4%) as a foam: [α]$_D$ +46.5 (*c* 0.2, chloroform). Anal. (C₂₇H₄₇N₃O₇S₂Si₂) C, H, N, S.

The slowest moving band gave **15b** (0.08 g, 31%) as a foam: [α]$_D$ −24.5 (*c* 0.5, chloroform). Anal. (C₂₇H₄₇N₃O₇S₂Si₂) C, H, N, S.

Methyl 5-*O*-Benzoyl-2-*O*-(*tert*-butyldimethylsilyl)-3-*C*-cyano-3-*O*-mesyl-D-ribofuranoside (18). A solution of cyanomesylate **16**[19] (0.5 g, 1.26 mmol) in a 9:1 mixture of trifluoracetic acid and H₂O (5 mL) was stirred at room temperature for 4 h. Volatiles were removed, and the residue was coevaporated with methanol (3 × 5 mL). The crude residue was then dissolved in methanol (10 mL), treated with concentrated H₂SO₄ (0.15 mL), and stirred at room temperature for 3 days. The solution was neutralized (pyridine), evaporated, and coevaporated with pyridine (2 × 5 mL) to afford **17** that was used in the next step without further purification. The crude containing **17** (0.42 g) was dissolved in dry acetonitrile (8 mL), and *tert*-butyldimethylsilyl chloride (TBDMSCl) (0.14 g) and DMAP (0.13 g) were added. The reaction mixture was stirred for 8 h at room temperature. Volatiles were removed, and the residue was treated with ethyl acetate and filtered. Purification by flash column chromatography (hexane−ethyl acetate, 4:1) gave **18** as a syrup (0.35 g, 57% from **16**): ¹H NMR (CDCl₃, 200 MHz) δ 3.03 (s, 3H, SO₂-CH₃), 3.28 (s, 3H, OCH₃), 4.55 (m, 4H, H-2, 2H-5), 4.80 (d, 1H, H-1, $J_{1,2}$ = 5.4 Hz), 7.60 (m, 5H, Ph). Anal. (C₂₁H₃₁NO₈SSi) C, H, N, S.

[Methyl 2,5-Bis-*O*-(*tert*-butyldimethylsilyl)-β-D-ribofuranoside]-3-spiro-5′-(4′-amino-1′,2′-oxathiole 2′,2′-Dioxide) (20). To a solution of **18** (0.3 g, 0.62 mmol) in dry acetonitrile (6 mL) was added DBU (0.092 mL, 0.62 mmol). The reaction was stirred at room temperature for 90 min. The solution was neutralized (acetic acid), and volatiles were removed. The residue was stirred in a saturated methanolic ammonia solution (20 mL) for 6 h. The solvent was evaporated to dryness. The crude was dissolved in dry acetonitrile (6 mL), and TBDMSCl (0.19 g) and DMAP (0.15 g) were added. The mixture was stirred at room temperature for 24 h. Volatiles were removed; the residue was treated with ethyl acetate (20 mL) and filtered. The residue was purified by flash column chromatography (hexane−ethyl acetate, 5:1) to give **20** (0.14 g, 45%, from **18**) as an amorphous solid: [α]$_D$ −17.5 (*c* 0.28, chloroform); ¹H NMR [(CD₃)₂CO, 300 MHz] δ 3.51 (s, 3H, OCH₃), 3.92 (m, 2H, H-5), 4.22 (t, 1H, H-4, $J_{4,5}$ = 2.3 Hz), 4.37 (d, 1H, H-2), 4.84 (d, 1H, H-1, $J_{1,2}$ = 5.3 Hz), 5.67 (s, 1H, H-3′), 6.29 (bs, 1H, NH₂-4′). Anal. (C₂₀H₄₁NO₇SSi₂) C, H, N, S.

Benzyl 2,5-Bis-*O*-(*tert*-butyldimethylsilyl)-3-*C*-cyano-3-*O*-mesyl-β-D-ribofuranoside (25 and 26). A solution of **21**[32] (1.43 g, 3 mmol) in CH₂Cl₂ (50 mL) containing pyridinium dichromate (0.8 g, 2.14 mmol) and acetic anhydride (1 mL, 9.41 mmol) was refluxed for 3 h. The solvent was evaporated, and

ethyl acetate (50 mL) was added, at which point the chromium complex precipitated. The mixture was passed quickly through a flash silica gel column with more ethyl acetate, and the colorless eluate was evaporated. The residues were coevaporated with ethanol (4 × 10 mL) and then with toluene (2 × 10 mL). The product (1.1 g, 95−98% purity, from ^{1}H NMR), ulose **22**, was used inmediately in the next step without further purification. Thus, crude ulose **22** (1.1 g, 2.3 mmol) was added to a rapidly stirred mixture containing NaCN (0.22 g, 4.6 mmol) and NaHCO$_3$ (0.39 g, 4.69 mmol) in H$_2$O (6 mL) and diethyl ether (12 mL). After 4 days at room temperature, the two phases were separated and extracted with diethyl ether (2 × 25 mL). The combined ethereal extracts were dried (Na$_2$SO$_4$), filtered, and evaporated to dryness. The residue, a mixture of the two epimeric cyanohydrins (**23** and **24**), was treated with mesyl chloride (0.86 mL, 11 mmol) in dry pyridine (26 mL) at 4 °C for 48 h. The mixture was poured into ice and water and extracted with CH$_2$Cl$_2$ (2 × 25 mL). The combined extracts were washed successively with 1 N HCl (25 mL), aqueous NaHCO$_3$ (25 mL), and brine (25 mL) and dried (NaSO$_4$). After evaporation of the solvent, the residue was purified by column chromatography (hexane−ethyl acetate, 18:1). The fastest moving fractions afforded **26** as a syrup (0.76 g, 60%): [α]$_D$ −46.2 (*c* 1, chloroform); ^{1}H NMR (CDCl$_3$, 200 MHz) δ 3.14 (s, 3H, SO$_2$CH$_3$), 3.90 (d, 2H, 2H-5), 4.49 (d, 1H, CHPh, *J* = 11.8 Hz), 4.57 (t, 1H, H-4, *J*$_{4,5}$ = 6.5 Hz), 4.76 (d, 1H, CHPh), 4.82 (s, 1H, H-2), 4.99 (s, 1H, H-1), 7.32 (m, 5H, Ph); ^{13}C NMR (CDCl$_3$, 50 MHz) δ 17.91, 18.22 (tBu), 40.19 (CH$_3$SO$_2$), 60.39 (C-5), 70.14 (OCH$_2$Ph), 80.91, 84.52 (C-2, C-4), 82.25 (C-3), 107.49 (C-1), 113.77 (CN), 128.04 (CH−Ar), 136.76 (C−Ar). Anal. (C$_{26}$H$_{45}$NO$_7$SSi$_2$) C, H, N, S.

The slowest moving fractions afforded **25** (0.19 g, 15%) as a syrup: [α]$_D$ +5 (*c* 1, chloroform); ^{1}H NMR (CDCl$_3$, 200 MHz) δ 3.12 (s, 3H, SO$_2$CH$_3$), 3.95 (dd, 2H, 2H-5), 4.00 (d, 1H, CHPh, *J* = 11.9 Hz), 4.53 (d, 1H, H-2), 4.56 (d, 1H, CHPh), 4.65 (m, 1H, H-4), 5.02 (d, 1H, H-1, *J*$_{1,2}$ = 4.2 Hz), 7.35 (m, 5H, Ph). Anal. (C$_{26}$H$_{45}$NO$_7$SSi$_2$) C, H, N, S.

[Benzyl 2,5-Bis-*O*-(*tert*-butyldimethylsilyl)-β-D-ribofuranoside]-3-spiro-5′-(4′-amino-1′,2′-oxathiole 2′,2′-Dioxide) (27). To a solution of **25** (0.1 g, 0.17 mmol) in dry acetonitrile (5 mL) was added DBU (0.029 mL, 0.19 mmol). The mixture was stirred at room temperature for 2 h, neutralized (acetic acid), and evaporated to dryness. The residue was purified by CCTLC on the chromatotron (hexane−ethyl acetate, 8:1) to give **27** (0.05 g, 50%) as a syrup: [α]$_D$ −61.6 (*c* 1, chloroform); ^{1}H NMR (CDCl$_3$, 200 MHz) δ 3.80 (m, 3H, H-4, 2H-5), 4.30 (d, 1H, H-2), 4.57 (d, 1H, CHPh, *J* = 11.3 Hz), 4.81 (d, 1H, CHPh), 5.08 (d, 1H, H-1, *J*$_{1,2}$ = 3.8 Hz), 5.49 (bs, 2H, NH$_2$-4′), 5.50 (s, 1H, H-3′), 7.24 (m, 5H, Ph); ^{13}C NMR (CDCl$_3$, 50 MHz) δ 25.98 (tBu), 65.11 (C-5), 72.00 (CH$_2$Ph) 76.61, 83.98, 92.39 (C-2, C-4, C-3′), 106.22 (C-1), 128.06 (CH−Ph), 136.61 (C−Ph), 151.03 (C-4′). Anal. (C$_{26}$H$_{45}$NO$_7$SSi$_2$) C, H, N.

[Benzyl 2,5-Bis-*O*-(*tert*-butyldimethylsilyl)-β-D-xylofuranoside]-3-spiro-5′-(4′-amino-1′,2′-oxathiole 2′,2′-Dioxide) (28). Following the method described for the synthesis of **27**, cyanomesyl derivative **26** (0.1 g, 0.17 mmol) was treated with DBU for 2 h. After the workup, the residue was purified by CCTLC on the chromatotron (hexane−ethyl acetate, 8:1) to give **28** (0.07 g, 70%) as a syrup: [α]$_D$ −8.8 (*c* 1, chloroform); ^{1}H NMR (CDCl$_3$, 200 MHz) δ 3.87 (d, 2H, H-5), 4.47 (d, 1H, H-2), 4.58 (m, 2H, H-4, CHPh, *J*$_{4,5}$ = 4.5 Hz), 4.78 (d, 1H, CHPh, *J* = 11.9 Hz), 5.06 (d, 1H, H-1, *J*$_{1,2}$ = 1.7 Hz), 5.58 (s, 1H, H-3′), 6.05 (bs, 1H, NH$_2$-4′), 7.35 (m, 5H, Ph); ^{13}C NMR (CDCl$_3$, 50 MHz) δ 25.66, 25.84 (tBu), 62.01 (C-5), 69.63 (CH$_2$-Ph), 83.42, 83.92 (C-2, C-4), 91.66 (C-3), 91.93 (C-3′), 107.27 (C-1), 128.21 (CH−Ph), 136.62 (C−Ph), 152.81 (C-4′). Anal. (C$_{26}$H$_{45}$NO$_7$SSi$_2$) C, H, N.

Modeling Methods. 1. Ab Initio Calculations. Both *N*[1]-methylthymine and the urea moiety present in **10b** in four alternative conformations were model-built in Insight-II.[45] Each molecule was fully optimized with the ab initio quantum mechanical program Gaussian 94[46] using the 3-21G* basis set. Atom-centered charges were then calculated on the optimized geometries employing a 6-31G* basis set.[47]

2. Similarity Calculations. The ASP (Automated Similarity Package) program[48] was used to compare the molecular electrostatic potentials (MEP) of *N*[1]-methylthymine (T) and the four different conformers of the acyclic analogue present in **10b** (U). A quantitative measure of the similarity (*S*) between the shapes of the charge distributions of two superimposed molecules, T and U, can be computed according to the following equation:[49]

$$S_{TU} = \frac{\int \rho_T \rho_U \, dv}{\sqrt{\int \rho_T^2 \, dv}\sqrt{\int \rho_U^2 \, dv}}$$

where ρ_T and ρ_U are the electron densities of molecules T and U, respectively. The numerator is a measure of the charge density for the two molecules, and the denominator is a normalization factor so that the function takes a range of values from 0 to 1, where 1 indicates identical electron densities. Calculated indices range from +1.0 (perfect similarity) to −1.0.

The similarity index was calculated by numerical integration of the MEPs over a three-dimensional grid of points separated by 0.25 Å and extending 10 Å beyond the bounds of the molecules. The MEPs were computed at each grid point (*r*) outside the van der Waals surface of the molecules by means of the following equation:

$$\text{MEP}(r) = \sum_{i=1}^{n} \frac{q_i}{r - r_i}$$

where q_i is the point charge on atom *i*, r_i is the position of atom *i*, and *n* is the number of charges in the molecule.

3. Automated Docking Procedure. To produce a relatively unbiased docking of both the thymine ring of TSAO-T and the abasic thymine analogue present in compound **10b**, the Monte Carlo simulated annealing technique implemented in AutoDock[50] was used. A reduced molecular model of the protein containing the binding site for nonnucleoside inhibitors was obtained from the X-ray coordinates of HIV-1 RT in its complex with nevirapine.[44] Rapid energy evaluation of each configuration explored was achieved by precalculating atomic affinity potentials for carbon, oxygen, nitrogen, and hydrogen atoms in the nonnucleoside binding site using a three-dimensional grid[51] centered on Leu-A100. An additional grid of electrostatic potential was calculated using a Poisson−Boltzmann finite difference method, as described below.

4. Continuum Electrostatics Calculations. Finite difference solutions to the linearized Poisson−Boltzmann equation,[52] as implemented in the DelPhi module of Insight-II,[45] were used to calculate the electrostatic potential in and around the nonnucleoside binding site of HIV-1 RT. Dielectric constant values assigned were 80.0 for the solvent (0.145 M) and 4.0 for the protein. The dielectric boundary was positioned at the solvent-accessible molecular surface,[53] calculated with a spherical probe of 1.4-Å radius, and a 2-Å thick ion exclusion layer was considered. Van der Waals parameters and point charges were taken from the AMBER[54] database.[55] To improve the accuracy of the calculated electrostatic potentials in the binding site, focusing[56] was done in three consecutive steps. A first cubic lattice was defined with 1.0-Å spacing and dimensions of 82 × 84 × 80 Å³ centered on the nonnucleoside binding pocket so as to leave a minimum separation of 35 Å between any protein atom and the borders of the box. The potentials at the grid points delimiting the first box were calculated analytically by treating each protein atom as a Debye−Hückel sphere.[42] A smaller (52 × 54 × 51 Å³) and finer grid (0.75-Å spacing) was then defined, the boundary potentials of which were linearly interpolated from those calculated in the previous run. This procedure was repeated in order to obtain the final grid (31 × 33 × 30 Å³) with 0.5-Å spacing.

Biological Methods. 1. Cells and Viruses. MT-4 cells were kindly provided by Dr. N. Yamamoto (Tokyo, Japan); CEM cells were obtained from the American Tissue Culture

Collection (Rockville, MD). HIV-1(III$_B$) was originally obtained from the culture supernatant of persistently HIV-1-infected H9 cells and was provided by Dr. R. C. Gallo and Dr. M. Popovic (National Institutes of Health, Bethesda, MD). HIV-2(ROD) was a kind gift of Dr. L. Montagnier (Pasteur Institute, Paris, France).

2. Sensitivity of Several HIV-1 Mutant Strains to Various Test Compounds in CEM and MT-4 Cells. CEM cells were suspended at 250 000 cells/mL of culture medium and infected with HIV-1(III$_B$) or HIV-2(ROD) at 100 times the 50% cell culture infective dose (CCID$_{50}$) (1 CCID$_{50}$ being the dose infective for 50% of the cell cultures)/mL of cell suspension. Then, 100 μL of the infected CEM cell suspension was added to 200-μL microtiter plate wells containing 100 μL of an appropriate dilution of the test compounds. After 4 days of incubation at 37 °C, the CEM cell cultures were examined for syncytium formation. The EC$_{50}$ was determined as the compound concentration required to inhibit syncytium formation by 50%. The CC$_{50}$ was determined as the compound concentration required to inhibit CEM cell proliferation by 50%.

MT-4 cells (5 $\times$ 10^5 cells/mL) were suspended in fresh culture medium and infected with HIV-1 or HIV-2 at 100 times the 50% CCID$_{50}$/mL of cell suspension. Then, 100 μL of the infected cell suspension was transferred to microtiter plate wells, mixed with 100 μL of the appropriate dilutions of the TSAO derivatives, and further incubated at 37 °C. After 5 days the number of viable cells was determined in a blood-cell-counting chamber by Trypan blue staining for both virus-infected and mock-infected cell cultures. The 50% effective concentration (EC$_{50}$) and 50% cytotoxic concentration (CC$_{50}$) were defined as the compound concentrations required to reduce by 50% the number of viable cells in the virus-infected and mock-infected cell cultures, respectively.

3. RT Enzyme Assay. The RT assays contained in a total reaction mixture volume (50 μL) 50 mM Tris·HCl (pH 7.8), 5 mM dithiothreitol, 300 mM glutathione, 500 μM EDTA, 150 mM KCl, 5 mM MgCl$_2$, 1.25 μg of bovine serum albumin, appropriate concentrations of labeled substrate [8-^{3}H]dGTP (specific radioactivity 15.6 Ci/mmol) (Moravek Biochemicals, Brea, CA), a fixed concentration of the template/primer poly(C)·oligo(dG)$_{12-18}$ (0.1 mM), 0.06% Triton X-100, 10 μL of inhibitor at various concentrations, and 1 μL of the RT preparation. The reaction mixtures were incubated at 37 °C for 15 min, at which time 100 μL of calf thymus DNA (150 μg/mL), 2 mL of Na$_4$P$_2$O$_7$ (0.1 M in 1 M HCl), and 2 mL of trichloroacetic acid (10% v/v) were added. The solutions were kept on ice for 30 min, after which the acid-insoluble material was washed and analyzed for radioactivity. In the experiments where the IC$_{50}$ values of the test compounds were determined with respect to [8-^{3}H]dGTP, a fixed concentration of the natural substrate [8-^{3}H]dGTP (2.5 μM) was used.

References

(1) Katz, R. A.; Skalka, A. M. The retroviral enzymes. *Annu. Rev. Biochem.* **1994**, *63*, 133–173.

(2) Vaishnav, Y. N.; Wong-Staal, F. The biochemistry of AIDS. *Annu. Rev. Biochem.* **1991**, *60*, 577–630.

(3) Schinazi, R. F. Competitive inhibitors of human immunodeficiency virus reverse transcriptase. *Perspect. Drug Discov. Des.* **1993**, *1*, 151–180.

(4) Young, S. D. Nonnucleoside inhibitors of HIV-1 reverse transcriptase. *Perspect. Drug. Discov. Des.* **1993**, *1*, 181–192.

(5) De Clercq, E. Towards improved anti-HIV chemotherapy: therapeutic strategies for intervention with HIV infections. *J. Med. Chem.* **1995**, *38*, 2491–2517.

(6) De Clercq, E. HIV-1 specific RT inhibitors: Highly selective inhibitors of human immunodeficiency virus type 1 that are specifically targeted at the viral reverse transcriptase. *Med. Res. Rev.* **1993**, *13*, 229–258.

(7) De Clercq, E. Nonnucleoside reverse transcriptase inhibitors (NNRTIs) for the treatment of human immunodeficiency virus type 1 (HIV-1) infections: strategies to overcome drug resistance development. *Med. Res. Rev.* **1996**, *16*, 125–157.

(8) Jacobo-Molina, A.; Ding, J.; Nanni, R. G.; Clark, A. D., Jr.; Lu, X.; Tantillo, C.; Williams, R. L.; Kamer, G.; Ferris, A. L.; Clark, P.; Hizi, A.; Hughes, S. H.; Arnold, E. Crystal structure of human immunodeficiency virus type 1 reverse transcriptase complexed with double-stranded DNA at 3.0 Å resolution shows bent DNA. *Proc. Natl. Acad Sci. U.S.A.* **1993**, *90*, 6320–6324. (b) Tantillo, C.; Ding, J.; Jacobo-Molina, A.; Nanni, R. G.; Boyer, P. L.; Hughes, S. H.; Pauwels, R.; Andries, K.; Janssen, P. A. J.; Arnold, E. Locations of anti-AIDS drug binding sites and resistance mutations in the three-dimensional structure of HIV-1 reverse transcriptase. Implications for mechanisms of drug inhibition and resistance. *J. Mol. Biol.* **1994**, *243*, 369–387.

(9) Nanni, R. G.; Ding, J.; Jacobo-Molina, A.; Hughes, S. H.; Arnold, E. Review of HIV-1 reverse transcriptase three-dimensional structure: Implications for drug design. *Perspect. Drug Discov. Des.* **1993**, *1*, 129–150.

(10) Smerdon, S. J.; Jäger, J.; Wang, J.; Kohlstaedt, L. A.; Chirino, A. J.; Friedman, J. M.; Rice, P. A.; Steitz, T. A. Structure of the binding site for nonnucleoside inhibitors of the reverse transcriptase of human immunodeficiency virus type 1. *Proc. Natl. Acad. Sci. U.S.A.* **1994**, *91*, 3911–3915.

(11) Balzarini, J.; Pérez-Pérez, M. J.; San-Félix, A.; Schols, D.; Perno, C. F.; Vandamme, A. M.; Camarasa, M. J.; De Clercq, E. 2′,5′-Bis-*O*-(*tert*-butyldimethylsilyl)-3′-spiro-5″-(4″-amino-1″,2″-oxathiole-2″,2″-dioxide)pyrimidine (TSAO) nucleoside analogues: Highly selective inhibitors of human immunodeficiency virus type 1 that are targeted at the viral reverse transcriptase. *Proc. Natl. Acad. Sci. U.S.A.* **1992**, *89*, 4392–4396. (b) Camarasa, M. J.; Pérez-Pérez, M. J.; San-Félix, A.; Balzarini, J.; De Clercq, E. 3′-Spironucleosides (TSAO derivatives), a new class of specific human immunodeficiency virus type 1 inhibitors: Synthesis and antiviral activity of 3′-spiro-5″-[4″-amino-1″,2″-oxathiole-2″,2″-dioxide]pyrimidine nucleosides. *J. Med. Chem.* **1992**, *35*, 2721–2727.

(12) Camarasa, M. J.; Pérez-Pérez, M. J.; Velázquez, S.; San-Félix, A.; Alvarez, A.; Ingate, S.; Jimeno, M. L.; Karlsson, A.; De Clercq, E.; Balzarini, J. TSAO derivatives: Highly specific inhibitors of human immunodeficiency virus type-1 (HIV-1) replication. *Nucleosides Nucleotides* **1995**, *14*, 585–594. (b) Balzarini, J.; Camarasa, M. J.; Karlsson, A. TSAO derivatives: Highly specific human immunodeficiency virus type 1 (HIV-1) reverse transcriptase inhibitors. *Drugs Future* **1993**, *18*, 1043–1055.

(13) Jonckheere, H.; Taymans, J. M.; Balzarini, J.; Velázquez, S.; Camarasa, M. J.; Desmyter, J.; De Clercq, E.; Anné, J. Resistance of HIV-1 reverse transcriptase against [2′,5′-bis-*O*-(*tert*-butyldimethylsilyl)-3′-spiro-5″-(4″-amino-1″,2″-oxathiole-2″,2″-dioxide)] (TSAO) derivatives is determined by the mutation Glu^{138} → Lys on the p51 subunit. *J. Biol. Chem.* **1994**, *269*, 25255–25258.

(14) Balzarini, J.; Kleim, J. P.; Riess, G.; Camarasa, M. J.; De Clercq, E.; Karlsson, A. Sensitivity of (138 GLU → LYS) mutated human immunodeficiency virus type 1 (HIV-1) reverse transcriptase (RT) to HIV-1-specific RT inhibitors. *Biochem. Biophys. Res. Commun.* **1994**, *201*, 1305–1312.

(15) Boyer, P. L.; Ding, J.; Arnold, E.; Hughes, S. H. Subunit specificity of mutations that confer resistance to nonnucleoside inhibitors in human immunodeficiency virus type 1 reverse transcriptase. *Antimicrob. Agents Chemother.* **1994**, *38*, 1909–1914.

(16) Balzarini, J.; Pérez-Pérez, M. J.; San-Félix, A.; Camarasa, M. J.; Bathurst, I. C.; Barr, P. J.; De Clercq, E. Kinetics of inhibition of human immunodeficiency virus type 1 (HIV-1) reverse transcriptase by the novel HIV-1 specific nucleoside analogue 2′,5′-bis-*O*-(*t*-butyldimethylsilyl)-3′-spiro-5″-(4″-amino-1″,2″-oxathiole-2″,2″-dioxide) thymine (TSAO-T). *J. Biol. Chem.* **1992**, *267*, 11831–11838.

(17) Alvarez, R.; Jimeno, M. L.; Pérez-Pérez, M. J.; De Clercq, E.; Balzarini, J.; Camarasa, M. J. Synthesis and anti-human immunodeficiency virus type 1 activity of novel 3′-spiro nucleoside analogues of TSAO-T. *Antiviral Chem. Chemother.* **1997**, *8*, 507–509.

(18) Balzarini, J.; Pérez-Pérez, M. J.; San-Félix, A.; Velázquez, S.; Camarasa, M. J.; De Clercq, E. [2′,5′-bis-*O*-(*tert*-butyldimethylsilyl)]-3′-spiro-5″-(4″-amino-1″,2″-oxathiole-2″,2″-dioxide) (TSAO) derivatives of purine and pyrimidine nucleosides as potent and selective inhibitors of human immunodeficiency virus type 1. *Antimicrob. Agents Chemother.* **1992**, *36*, 1073–1080.

(19) Pérez-Pérez, M. J.; San-Félix, A.; Balzarini, J.; De Clercq, E.; Camarasa, M. J. TSAO analogues. Stereospecific synthesis and anti-HIV-1 activity of 1-[2′,5′-bis-*O*-(*tert*-butyldimethylsilyl-β-D-ribofuranosyl)-3′-spiro-5″-[4″-amino-1″,2″-oxathiole-2″,2″-dioxide]pyrimidine and pyrimidine modified nucleosides. *J. Med. Chem.* **1992**, *35*, 2988–2995.

(20) Velázquez, S.; San-Félix, A.; Pérez-Pérez, M. J.; Balzarini, J.; De Clercq, E.; Camarasa, M. J. TSAO Analogues. 3. Synthesis and anti-HIV-1 activity of [2′,5′-bis-*O*-(*tert*-butyldimethylsilyl-β-D-ribofuranosyl)-3′-spiro-5″-[4″-amino-1″,2″-oxathiole-2″,2″-dioxide] purine and purine-modified nucleosides. *J. Med. Chem.* **1993**, *36*, 3230–3239.

(21) Alvarez, R.; Velázquez, S.; San-Félix, A.; Aquaro, S.; De Clercq, E.; Perno, C.-F.; Karlsson, A.; Balzarini, J.; Camarasa, M. J. 1,2,3-Triazole-[2′,5′-bis-*O*-(*tert*-butyldimethylsilyl-β-d-ribofuranosyl]-3′-spiro-5″-(4″-amino-1″,2″-oxathiole-2″,2″-dioxide) (TSAO) analogues. Synthesis and anti-HIV-1 activity. *J. Med. Chem.* **1994**, *37*, 4185–4194.

(22) A preliminary account of this work was presented at the Eleventh International Conference on Antiviral Research, San Diego, CA, April 5–10, 1998; Abstract 43; *Antitiviral Res.* **1998**, *37* (3), A53.

(23) Gololobov, Y. G.; Kasukhin, L. F. Recent advances in the Staudinger reaction. *Tetrahedron* **1992**, *48*, 1353–1406.

(24) Paulsen, H.; Pflughaupt, K. W. Glycosylamines. In *The Carbohydrates Chemistry and Biochemistry*, 2nd ed.; Pigman, W., Horton, D., Eds.; Academic Press: New York, 1980; pp 881–921.

(25) Bognár, R.; Nánási, P.; Lipták, A. Preparation of isomeric *N*-arylglucopyranosylamine tetramethyl ethers (*N*-glycosides. XII). *Acta Chim. Hung.* **1965**, *45*, 47–54.

(26) Collins, P. M.; Ferrier, R. J. *Monosaccharides. Their chemistry and their roles in natural products;* John Wiley and Sons Ltd.; Chichester, 1995; pp 126–134.

(27) Ewing, D. F.; Humble, R. W.; Mackenzie, G. NMR studies of configuration and conformation in *N*-acyl-D-ribosylamines. *J. Carbohydr. Chem.* **1991**, *10*, 387–397.

(28) Ewing, D. F.; Hiebl, J.; Humble, R. W.; Mackenzie, G.; Raynor, A.; Zbiral, E. Stereoselctive synthesis of *N*-(α- and β-ribofuranosyl)-formamides and related glycosyl formamides -precursors of sugar isocyanates. *J. Carbohydr. Chem.* **1993**, *12*, 923–932.

(29) Kuhn, R.; Kirschenlohr, W. β-Glycosides of *N*-acetyl-D-glucosamine. *Annal* **1956**, *600*, 115–125. (b) Galbis-Pérez, J. A.; Pinto-Corraliza, R. M.; Román-Galán, E.; Gómez-Guillén, M. Síntesis de 2-amino-2-desoxi-hexosas por el método del aminonitrilo. *An. Chim.* **1979**, *75*, 387–391. (c) Avalos, M.; Babiano, R.; Cintas, P.; Jiménez, J. L.; Palacios, J. C.; Valencia, C. Condensation of 2-amino-2-deoxysugars with isocyanates. Synthesis of *cis*-1,2-fused glycopyrano heterocycles. *Tetrahedron* **1994**, *50*, 3273–3296.

(30) Hronowski, L. J. J.; Szarek, W. A. Synthesis of cyclopentane analogues of 1-(2′- and 3′-dideoxy-β-*erythro*-pentofuranosyl and ribofuranosyl)-2-thiouracil nucleosides. *Can. J. Chem.* **1986**, *64*, 1620–1629.

(31) Hronowski, L. J. J.; Szarek, W. A. Synthesis of cyclopentane analogues of 1-(2′,3′-dideoxy-β-*glycero*-pentofuranosyl)pyrimidine nucleosides. *Can. J. Chem.* **1988**, *66*, 61–70.

(32) Avalos, M.; Babiano, R.; Cintas, P.; Jiménez, J. L.; Palacios, J. C.; Valencia, C. The reaction of 2-amino-2-deoxyhexopyranoses with isocyanates. Synthesis of ureas and their transformation into heterocyclic derivatives. *Tetrahedron* **1993**, *49*, 2655–2675.

(33) Nawrot, B.; Pankiewicz, K. W.; Zepf, R. A.; Watanabe, K. A. Synthesis and reactivity of benzyl 2-*O*-trifluoromethyl-sulfonyl and benzyl-3-*O*-trifluoromethylsulfonyl-β-D-ribofuranoside -the first evidence of trifluoromethyl-sulfonyl (triflyl) migration in carbohydrates. *J. Carbohydr. Chem.* **1988**, *7*, 95–114.

(34) Hollemberg, D. H.; Klein, R. S.; Fox, J. J. Pyridinium dichromate for the oxidation of carbohydrates. *Carbohydr. Res.* **1987**, *67*, 491–494.

(35) Calvo-Mateo, A.; Camarasa, M. J.; Díaz-Ortiz, A.; De las Heras, F. G. Novel aldol-type cyclocondensation of *O*-mesyl(methylsulphonyl)cyano-hydrins. Application to the stereospecific synthesis of branched-chain sugars. *J. Chem. Soc., Chem. Commun.* **1988**, 1114–1115.

(36) Pérez-Pérez, M. J.; Camarasa, M. J.; Díaz-Ortiz, A.; San Félix, A.; De las Heras, F. G. Stereospecific synthesis of branched-chain sugars by a novel aldol-type cyclocondensation. *Carbohydr. Res.* **1991**, *216*, 399–411.

(37) Stott, K.; Stonehouse, J.; Keeler, J.; Hwang, T. L.; Saka, A. J. Excitation sculpting in high-resolution nuclear magnetic resonance spectroscopy: application to selective NOE experiments. *J. Am. Chem. Soc.* **1995**, *117*, 4199–4200.

(38) Scheweizer, M. P.; Witkowsky, J.; Robins, R. K. Nuclear magnetic resonance determination of syn and anti conformations in pyrimidine nucleosides. *J. Am. Chem. Soc.* **1971**, *93*, 277–

279. (b) Ewing, D. F.; Humble, R. W.; Mackenzie, G. NMR studies of N¹- and N³-(D-2′-deoxyribofuranosyl) nucleosides from ethyl 5-aminoimidazole-4-carboxylate. *Nucleosides Nucleotides* **1991**, *10*, 1305–1316. (c) Kumar, A.; Katti, S. B.; Rosemeyer, H.; Seela, F. Conformational analysis of 3′-deoxyribonucleosides using 1D-NOE difference spectroscopy. *Nucleosides Nucleotides* **1996**, *15*, 1595–1601.

(39) Alvarez, R.; Jimeno, M. L.; Gago, F.; Balzarini, J.; Pérez-Pérez, M J.; Camarasa, M. J. Novel 3′-spiro nucleoside analogues of TSAO-T. Part II. A comparative study based on NMR conformational analysis in solution and theoretical calculations. *Antiviral Chem. Chemother.* **1998**, *9* (4), in press.

(40) Velázquez, S.; Alvarez, R.; San-Félix, A.; Jimeno, M. L.; De Clercq, E.; Balzarini, J.; Camarasa, M. J. Synthesis and anti-HIV-1 activity of [AZT]-[TSAO-T] and [AZT]-[HEPT] dimers as potential multifunctional inhibitors of HIV-1 reverse transcriptase. *J. Med. Chem.* **1995**, *38*, 1641–1649.

(41) Esnouf, R. M.; Ren, J.; Hopkins, A. L.; Ross, C. K.; Jones, E. Y.; Stammers, D. K.; Stuart, D. I. Unique features in the structure of the complex between HIV-1 reverse transcriptase and the bis-(heteroaryl)piperazine (BHAP) U-90152 explain resistance mutations for this nonnucleoside inhibitor *Proc. Natl. Acad. Sci. U.S.A.* **1997**, *94*, 3984–3989.

(42) Klapper, I.; Hagstrom, R.; Fine, R.; Sharp, K.; Honig, B. Focusing of electric fields in the active site of Cu−Zn superoxide dismutase: effects of ionic strength and amino acid modification. *Proteins* **1986**, *1*, 47–59.

(43) Pérez, C.; Gago, F.; Camarasa, M. J. Unpublished results.

(44) Ren, J. S.; Esnouf, R.; Garman, E.; Jones, Y.; Somers, D.; Ross, C.; Kirby, I.; Keeling, J.; Darby, G.; Stuart, D.; Stammers, D. High-resolution structure of HIV-1 RT: insights from four RT-inhibitor complexes. *Nature Struct. Biol.* **1995**, *2*, 293–302.

(45) Insight-II, release 95.0; Biosym/Molecular Simulations, 9685 Scranton Rd, San Diego, CA 92121-3752; 1995.

(46) Frisch, M. J.; Trucks, G. W.; Schlegel, H. B.; Gill, P. M. W.; Johnson, B. G.; Robb, M. A.; Cheeseman, J. R.; Keith, T.; Petersson, G. A.; Montgomery, J. A.; Raghavachari, K.; Al-Laham, M. A.; Zakrzewski, V. G.; Ortiz, J. V.; Foresman, J. B.; Cioslowski, J.; Stefanov, B. B.; Nanayakkara, A.; Challacombe, M.; Peng, C. Y.; Ayala, P. Y.; Chen, W.; Wong, M. W.; Andrés, J. L.; Replogle, E. S.; Gomperts, R.; Martin, R. L.; Fox, D. J.; Binkley, J. S.; Defrees, D. J.; Baker, J.; Stewart, J. P.; Head-Gordon, M.; González, C.; Pople, J. A. Gaussian 94, revision E.2; Gaussian, Inc., Pittsburgh, PA; 1995.

(47) Besler, B. H.; Merz, K. M.; Kollman, P. A. Atomic Charges Derived from Semiempirical Methods. *J. Comput. Chem.* **1990**, *11*, 431–439.

(48) Burt, C.; Huxley, P.; Richards, W. G. The application of molecular similarity calculations. *J. Comput. Chem.* **1990**, *11*, 1139–1146.

(49) Carbó, R.; Leyda, L.; Arnau, M. An electron density measure of the similarity between two compounds. *Int. J. Quantum Chem.* **1980**, *17*, 1185–1189.

(50) Goodsell, D. S.; Olson, A. J. Automated Docking of Substrates to Proteins by Simulated Annealing. *Proteins: Struct. Funct. Genet.* **1990**, *8*, 195–202. (b) Goodsell, D. S.; Morris, G. M.; Olson, A. J. Docking of Flexible Ligands: Applications of AutoDock. *J. Mol. Recognit.* **1996**, *9*, 1–5. (c) Morris, G. M.; Goodsell, D. S.; Huey, R.; Olson, A. J. AutoDock: Automated Docking of Flexible Ligands to Receptors, version 2.4; The Scripps Research Institute, La Jolla, CA 92037-5025; 1996.

(51) Goodford, P. J. A Computational Procedure for Determining Energetically Favorable Binding Sites on Biologically Important Macromolecules. *J. Med. Chem.* **1985**, *28*, 849–857.

(52) Nicholls, A.; Honig, B. A. Rapid Finite Difference Algorithm, Utilizing Successive Over-Relaxation to Solve the Poisson−Boltzmann Equation. *J. Comput. Chem.* **1991**, *12*, 435–445.

(53) Connolly, M. L. Analytical Molecular Surface Calculation *J. Appl. Crystallogr.* **1983**, *16*, 548–558.

(54) AMBER (UCSF): Assisted Model Building with Energy Refinement, version 4.1; Department of Pharmaceutical Chemistry, University of California, San Francisco, CA; 1995.

(55) Cornell, W. D.; Cieplak, P.; Bayly, C. I.; Gould, I. R.; Merz, K. M.; Ferguson, D. M.; Spellmeyer, D. C.; Fox, T.; Caldwell, J. W.; Kollman, P. A. A Second Generation Force Field for the Simulation of Proteins, Nucleic Acids, and Organic Molecules. *J. Am. Chem. Soc.* **1995**, *117*, 5179–5197.

(56) Gilson, M. K.; Sharp, K. A.; Honig, B. H. Calculating the Electrostatic Potential of Molecules in Solution: Method and Error Assessment. *J. Comput. Chem.* **1987**, *9*, 327–335.